Acta Crystallographica Section B
**Structural Science**
ISSN 0108-7681

# Superspace-symmetry determination and multi-dimensional refinement of the incommensurately modulated structure of natural fresnoite

**Luca Bindi,[a]* Michal Dusek,[b] Vaclav Petricek[b] and Paola Bonazzi[a]**

[a]Dipartimento di Scienze della Terra, Università di Firenze, Via La Pira 4, I-50121 Firenze, Italy, and [b]Institute of Physics, Academy of Sciences of the Czech Republic, Na Slovance 2, 182 21 Praha, Czech Republic

Correspondence e-mail: lbindi@geo.unifi.it

Received 4 April 2006
Accepted 1 August 2006

The structure of natural fresnoite, $Ba_2TiSi_2O_8$, from the sanbornite deposits of eastern Fresno County, California, has been solved and refined as an incommensurate structure in five-dimensional superspace. The structure is tetragonal, superspace group $P4bm(\alpha, \alpha, 1/2)(-\alpha, \alpha, 1/2)0gg$, cell parameters $a$ = 8.5353 (6), $c$ = 10.4128 (7) Å, modulation vectors $\mathbf{q}_1 = 0.3020\,(3)\,(\mathbf{a}^* + \mathbf{b}^*)$, $\mathbf{q}_2 = 0.3020\,(3)\,(-\mathbf{a}^* + \mathbf{b}^*)$. Data collection was performed on an Xcalibur CCD diffractometer at 110 K. The structure was refined from 3452 reflections to final $R$ = 0.0123. The model includes modulation of both atomic positions and displacement parameters. As a consequence of the Ba and O positional modulation, eight-, nine- and tenfold Ba coordinations occur throughout the structure. The change of coordination around the Ba atom is clearly represented by the deformation of the pentagonal rings, as seen from a projection along [001]. The deformed pentagonal rings correspond to Ba atoms with eight- and ninefold coordinations and form octagonal clusters closely resembling those observed in the incommensurate structure of melilite-type compounds.

## 1. Introduction

Fresnoite, $Ba_2TiSi_2O_8$, is structurally related to the melilite group minerals. The parent structure, space group $P4bm$, consists of a two-dimensional linkage of corner-sharing $TiO_5$ pyramids and $Si_2O_7$ groups (Masse *et al.*, 1967; Moore & Louisnathan, 1969). In the stacking of successive layers along [001], the tenfold-coordinated Ba cations are located about halfway between adjacent sheets. Fresnoite-type compounds having the chemical formulae $Ba_2TiSi_2O_8$ (BTS), $Ba_2TiGe_2O_8$ (BTG), $Sr_2TiSi_2O_8$ (STS) and $Ba_2VSi_2O_8$ (BVS) are of interest for their piezoelectric and pyroelectric properties (Kimura *et al.*, 1973; Schmid *et al.*, 1978; Iijima *et al.*, 1981; Halliyal *et al.*, 1985; Markgraf *et al.*, 1985), whereas the fresnoite-type $A_2V_3O_8$ ($A$ = K, Rb and $NH_4$) compounds have recently received much attention because of their low-temperature magnetic properties and their nonlinear optical behaviour (Liu & Greedan, 1995; Ye *et al.*, 1998; Choi *et al.*, 2002). The existence of different, closely related types of incommensurate modulations at room temperature in synthetic BTS, BTG and STS has recently been recognized (Markgraf & Bhalla, 1989; Markgraf *et al.*, 1990; Höche *et al.*, 1999). Markgraf *et al.* (1990), by means of an electron diffraction study, concluded that the modulation in BTS occurs along [100] and in the $hk\frac{1}{2}$ level. Withers *et al.* (2002), however, reinvestigated the incommensurate (IC) structure of BTS by means of electron

© 2006 International Union of Crystallography
Printed in Great Britain – all rights reserved

**Table 1**
Electron microprobe data (means and ranges in wt% of oxides), and atomic ratios with their standard deviations ($\sigma$) for the selected fresnoite crystal.

| | wt% | Range | Atomic ratios | $\sigma$ |
|---|---|---|---|---|
| BaO | 59.60 | 61.25–57.99 | 1.962 | 0.08 |
| $TiO_2$ | 15.83 | 14.81–16.11 | 1.000 | 0.06 |
| CaO | 0.43 | 0.10–0.88 | 0.038 | 0.01 |
| $SiO_2$ | 23.81 | 22.13–24.56 | 2.000 | 0.06 |
| Total | 99.67 | 99.42–100.63 | | |

microscopy and pointed out that the primary modulation wavevector has a $c^*/2$ commensurate component and an incommensurate component that runs along the $\langle 110\rangle_p^*$ direction(s) (where the subscript $p$ denotes the parent structure). Moreover, to obtain an insight into the mechanisms responsible for the incommensurate modulation in BTS, Withers *et al.* (2002) presented a rigid unit mode (RUM) analysis of the inherent displacive structural flexibility of the ideal framework of the fresnoite structure type. According to these authors, a key role in the stabilization of the IC structures observed in the fresnoite-type compounds is played by one RUM type involving the rotation of the constituent rigid tetrahedra and square pyramids around **c** and associated with the wavevector $\mathbf{q} \simeq 0.30\langle 110\rangle_p^*$. This hypothesis has been corroborated by the recent four-dimensional crystal structure refinement of synthetic $Ba_2TiGe_2O_8$ carried out by Höche *et al.* (2003), as well as by the combined temperature-dependent electron and single-crystal X-ray diffraction study of synthetic $Rb_2V^{4+}V_2^{5+}O_8$ (Withers *et al.*, 2004).

To date, the presence of an incommensurate modulation has never been observed in natural fresnoites. This is probably due to the minor isomorphic substitutions usually present in natural crystals. However, because of the scarcity of the studies of natural fresnoites, stabilization of the incommensurate structure in these crystals cannot be discarded. We report here the superspace-symmetry determination and the (3 + 2)-dimensional refinement of the incommensurately modulated structure of a natural fresnoite crystal.

## 2. Occurrence and chemical composition

The sample containing the fresnoite crystal used in the present study (Museo di Storia Naturale, Sezione di Mineralogia e Litologia, Università di Firenze, Italy, catalogue number 44362/G) is from the sanbornite deposits of eastern Fresno County, California.

A preliminary chemical analysis using energy-dispersive spectrometry, performed on the same crystal fragment used for the structural study, did not indicate the presence of elements ($Z > 9$) other than Ba, Ti, Ca and Si. The chemical composition was then determined using wavelength dispersive analysis (WDS) by means of a Jeol-JXA 8600 electron microprobe. Major and minor elements were determined at 20 kV accelerating voltage and 40 nA beam current, with a counting time of 30 s. For the WDS analyses the following lines were used: Ba $K\alpha$, Ti $K\alpha$, Ca $K\alpha$, Si $K\alpha$. The estimated analytical precision is $\pm$ 0.60 for Ba, $\pm$ 0.40 for Ti and Si, and $\pm$ 0.05 for Ca. The standards employed were baryte (Ba), rutile (Ti) and diopside (Ca, Si). The fresnoite fragment was found to be homogeneous within analytical error. The average chemical composition (five analyses on different spots), together with ranges of wt% of oxides, is reported in Table 1. On the basis of five cations, the formula can be written as $(Ba_{1.962}Ca_{0.038})_{\Sigma\,=\,2.000}Ti_{1.000}Si_{2.000}O_{8.000}$.

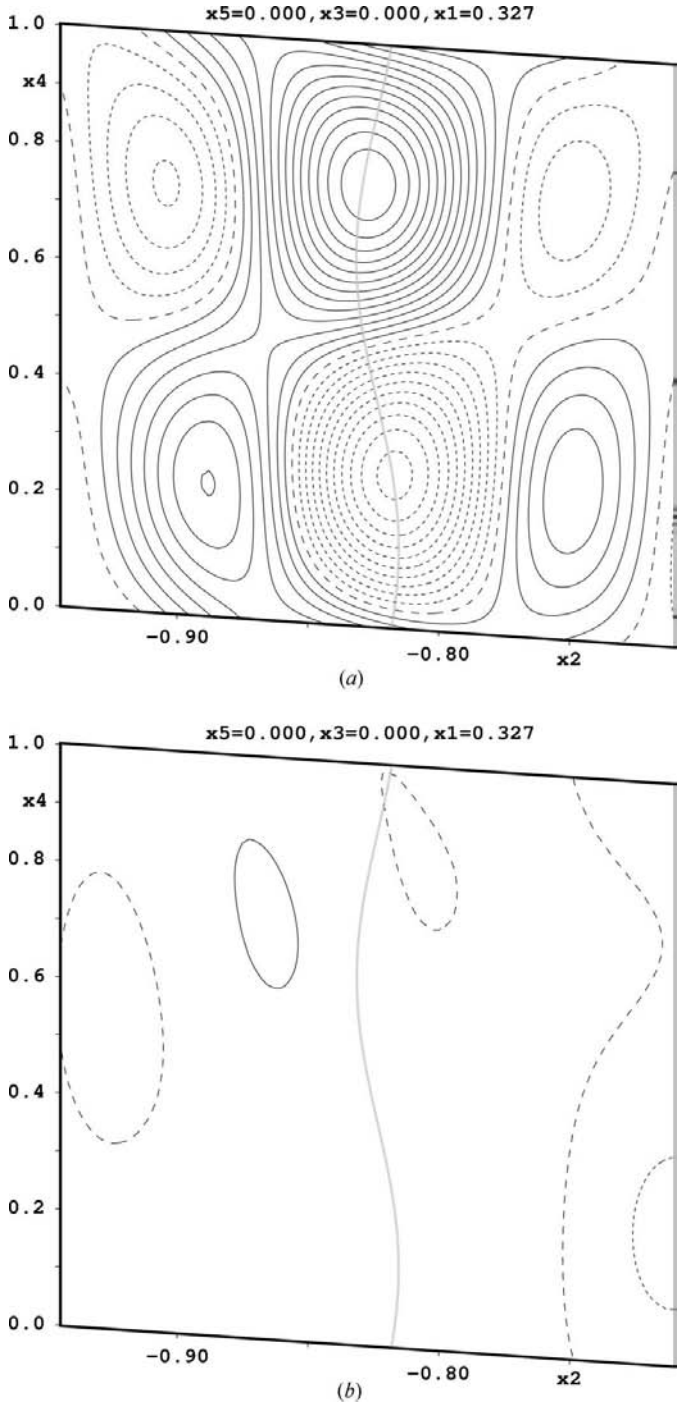


**Figure 1**
Electron density maps through the atomic position of Ba calculated (*a*) before and (*b*) after introducing anisotropic displacement parameter modulation. Contour interval 0.2 $e^-$ Å$^{-3}$. Negative contours dashed.

**Table 2**
Crystallographic data for the selected fresnoite crystal.

| | |
|---|---|
| Crystal data | |
| Chemical formula | $(Ba_{1.962}Ca_{0.038})O_{8.000}Si_{2.000}Ti_{1.000}$ |
| $M_r$ | 506.7 |
| Cell setting, superspace group | Tetragonal, $P4bm(\alpha,\alpha,1/2)(-\alpha,\alpha,\frac{1}{2})0gg$ |
| Temperature (K) | 110 |
| $a$, $c$ (Å) | 8.5353 (6), 10.4128 (7) |
| $V$ (Å$^3$) | 758.59 (9) |
| $Z$ | 4 |
| $D_x$ (Mg m$^{-3}$) | 4.435 |
| Radiation type | Mo $K\alpha$ |
| $\mu$ (mm$^{-1}$) | 11.67 |
| Crystal form, colour | Irregular, yellow |
| Crystal size (mm) | 0.09 × 0.06 × 0.03 |
| | |
| Data collection | |
| Diffractometer | Oxford Diffraction Xcalibur |
| Data collection method | $\omega$ scans |
| Absorption correction | Gaussian |
| $T_{min}$ | 0.314 |
| $T_{max}$ | 0.520 |
| No. of measured, independent and observed reflections | 43094, 3452, 2554 |
| No. of main reflections | 434 |
| No. of satellite reflections for ±(1,0), ±(0,1) | 1458 |
| No. of satellite reflections for ±(1,1), ±(1,−1) | 1560 |
| Criterion for observed reflections | $I > 3\sigma(I)$ |
| $R_{int}$ | 0.030 |
| $\theta_{max}$ (°) | 36.1 |
| | |
| Refinement | |
| Refinement on | $F$ |
| $R[F > 2\sigma(F)]$, $wR(F)$, $S$ | 0.012, 0.018, 0.94 |
| $R$, $wR$ (all reflections) | 0.012, 0.017 |
| $R$, $wR$ (main reflections) | 0.010, 0.010 |
| $R$, $wR$ (satellites) for ±(1,0), ±(0,1) | 0.014, 0.016 |
| $R$, $wR$ (satellites) for ±(1,1), ±(1,−1) | 0.034, 0.041 |
| $S$ (obs), $S$ (all) | 1.08, 0.94 |
| No. of reflections | 3452 reflections |
| No. of parameters | 259 |
| H-atom treatment | No H atoms present |
| Weighting scheme | $w = 1/[\sigma^2(F) + 0.0001F^2]$ |
| $(\Delta/\sigma)_{max}$ | 0.028 |
| $\Delta\rho_{max}$, $\Delta\rho_{min}$ (e Å$^{-3}$) | 0.27, −0.32 |
| Absolute structure | Flack (1983), *JANA2000* (Petricek *et al.*, 2000). |
| Flack parameter | 0.932 (9) |

Computer programs used: *CrysAlisPro CCD* (Oxford Diffraction, 2004), *CrysAlisPro RED* (Oxford Diffraction, 2004), *SIR*2002 (Burla *et al.*, 2003), *JANA*2000 (Petricek *et al.*, 2000).

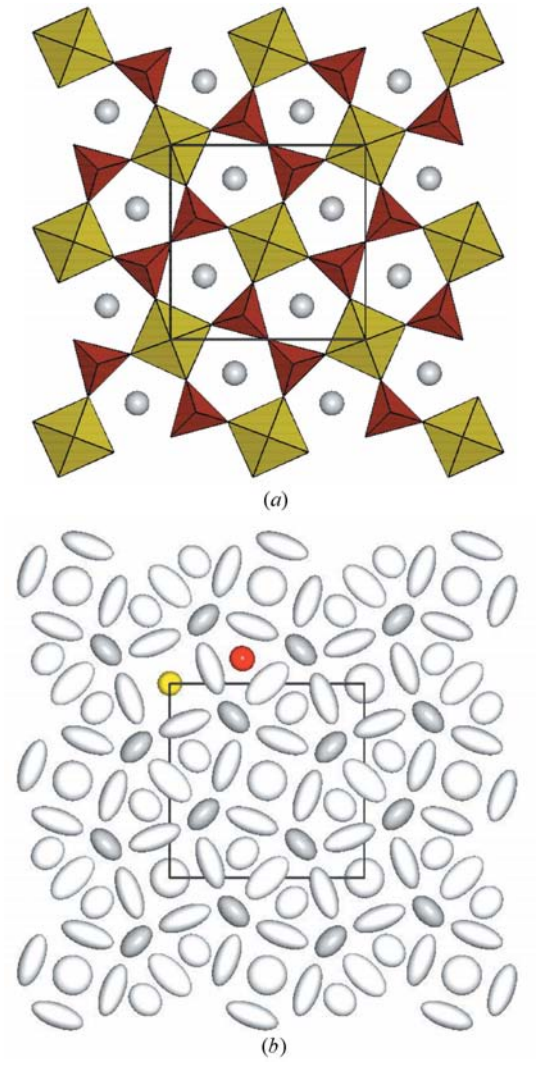


**Figure 2**
[001] projection of the average crystal structure of fresnoite: (*a*) the interconnection of $TiO_5$ pyramids (in light grey and yellow on-line) and $Si_2O_7$ groups (in dark grey and red on-line); grey represents Ba atoms; (*b*) displacement ellipsoids (95% probability level).

## 3. Experimental

A fresnoite crystal was selected from the 44362/G sample and examined preliminarily by means of an Enraf–Nonius CAD-4 single-crystal diffractometer equipped with a conventional point detector (Mo $K\alpha$ radiation) to check the diffraction quality. The same crystal was then mounted on an Oxford Diffraction Xcalibur version 2 diffractometer, fitted with a Sapphire 2 CCD detector. At room temperature a long exposure (100 s, 40 mA, 40 kV; Mo $K\alpha$ radiation) did not reveal any reflections other than those belonging to the basic structure. The measurement was then repeated at 110 K and the IC satellites were observed. Low-temperature X-ray diffraction data collection was carried out using a conventional X-ray tube with standard collimator and a very fine $\omega$ step of 0.25°. For the main measurement the exposure was 240 s deg$^{-1}$. The temperature of *ca* 110 K was achieved by means of a nitrogen gas Oxford Cryojet cooler. As already observed in the synthetic $Sr_2TiSi_2O_8$ (Höche *et al.*, 2002) and for $Ba_2TiSi_2O_8$ (Withers *et al.*, 2002), the modulation appeared to be two-dimensional, with modulation vectors $\mathbf{q}_1 = \alpha(\mathbf{a}^* + \mathbf{b}^*)$ and $\mathbf{q}_2 = \alpha(-\mathbf{a}^* + \mathbf{b}^*)$. The coefficient $\alpha = 0.3020(3)$ was determined by the least-squares method from 13 890 satellites. All reflections observed on collected frames were indexed by five *hklmn* integers and with respect to the five-dimensional base (de Wolff, 1974) $\mathbf{h} = h\mathbf{a}^* + k\mathbf{b}^* + l\mathbf{c}^* + m\mathbf{q}_1 + n\mathbf{q}_2$, where $\mathbf{a}^*$, $\mathbf{b}^*$ and $\mathbf{c}^*$ are the reciprocal axes of the basic structure. The integration of reflections and Lp, and absorption correction were performed

using *CrysAlisPro RED* (Oxford Diffraction, 2004). Table 2 shows the experimental details.[1]

## 4. Structure determination

### 4.1. Refinement of the average structure

The average structure was refined in the space group *P*4*bm* starting from the positional parameters of natural fresnoite reported by Moore & Louisnathan (1969). Since the chemical composition is close to that of the pure fresnoite $Ba_2TiSi_2O_8$, occupancy factors were constrained to unity. The scattering curves of neutral Ba, Ti, Si and O were used. The refinement quickly converged to $R = 0.0099$ for all the 434 main reflections. The influence of absolute structure was clearly detectable at this point as the inverted structure had $R = 0.0179$. The shape of the refined anisotropic displacement parameters of Ba and all O atoms revealed a strong in-plane smearing indicating possible modulations.

### 4.2. Refinement of the modulated structure

The Laue class (4/*mmm*) and reflection conditions (*hklmn*, $l + m + n = 2n$; $h0lm\bar{m}$, $h = 2n$; $0klnn$, $k + n + n = 2n$; $\bar{k}klm0$, $m = 2n$; $kkl0n$, $k + k + n = 2n$) led to the choice of the superspace group $P4bm(\alpha, \alpha, 1/2)(-\alpha, \alpha, 1/2)0gg$, in keeping with the previously reported structure of synthetic $Sr_2TiSi_2O_8$ (Höche *et al.*, 2002). Owing to its periodicity in superspace, each parameter of the modulated structure can be expressed as an expansion of a Fourier synthesis

$$p^{\mu}(x_4, x_5) = \sum_n \sum_m \left[p^{\mu}_{snm} \sin(2\pi n x_4 + 2\pi m x_5) + p^{\mu}_{cnm} \cos(2\pi n x_4 + 2\pi m x_5)\right],$$

where $x_4 = \mathbf{q}_1\mathbf{r}^{\mu} + t$, $x_5 = \mathbf{q}_2\mathbf{r}^{\mu} + u$, and $t$ and $u$ are internal phases. Only terms having $0 \leq n \leq 1$ and $-1 \leq m \leq 1$ were used in the refinement.

The refinement of the positional modulation of the atoms converged smoothly to $R = 0.0258$ for all reflections. The consecutive difference-Fourier maps revealed large minima and maxima close to the Ba atom. The most probable explanation is that, in some regions, the distribution of the Ba atom around its refined central position is more dispersed, while it is more concentrated in other regions. This feature could also indicate split atomic positions, but with the current resolution they could not be distinguished from a continuous distribution. A similar effect was also detected for atom O1. Therefore, in the final refinement, the modulation of the displacement parameters of all atoms was taken into account. This refinement converged to $R = 0.0123$, thus indicating that the modulation of the displacement parameters is highly significant. As an example, the residual electron density through the atomic position of Ba is shown before (Fig. 1*a*) and after (Fig. 1*b*) introducing anisotropic displacement parameter modulation. The refined positional parameters and their modulations, and the anisotropic displacement parameters and their modulations are given in the supplementary data,[1] while the interatomic distances together with bond-valence sums are given in Table 3.

## 5. Discussion

As is well known, the modulated character of a structure can be easily evaluated by the analysis of the size and the shape of the anisotropic displacement parameters of the average structure. The reason is that the strong anisotropy could reflect disorder related to the modulated character of the fine structure. If we consider the average structure of natural fresnoite projected down the *c* axis (Fig. 2), strongly anisotropic displacement parameters are observed for the O (especially for atoms O1 and O3) and Ba atoms, whereas the displacement ellipsoids for Ti and Si are approximately isotropic. The strong anisotropy observed for atoms O1, O3 and Ba is caused by a displacive modulation superimposed over the average structure and is in agreement with the results obtained with the five-dimensional crystal structure refinement described below.

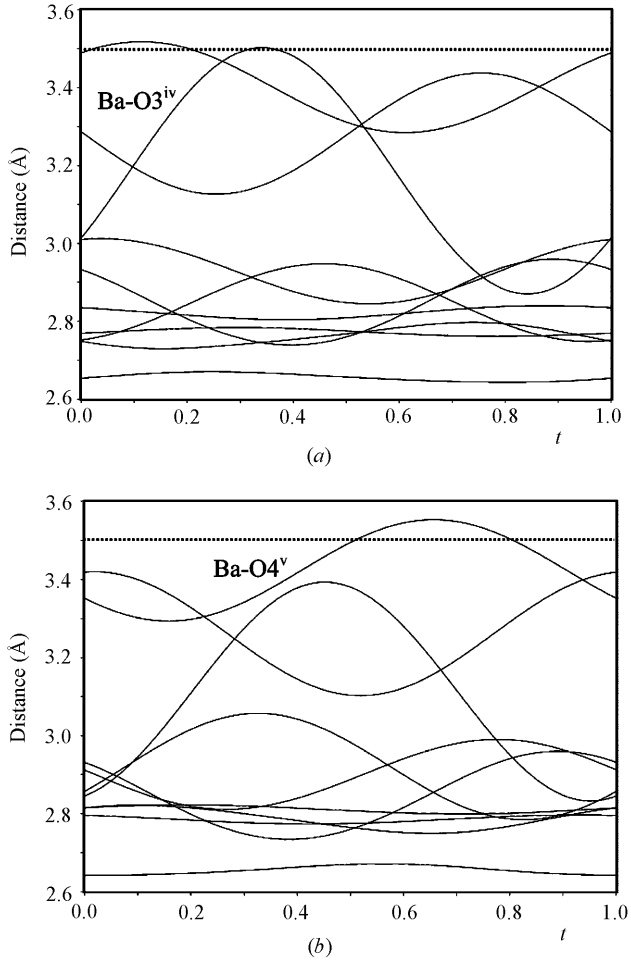


**Figure 3**
Variation of the Ba—O distances as functions of $t$ (*a*) at $u = 0.34$ and (*b*) at $u = 0.00$.

[1] Supplementary data for this paper are available from the IUCr electronic archives (Reference: CK5019). Services for accessing these data are described at the back of the journal.

As found for the IC structures of melilite-type compounds (Kusaka *et al.*, 2001; Bindi *et al.*, 2001, and references therein), in the case of fresnoite the most important variations observed as a function of the fourth ($t$) and the fifth ($u$) coordinate in the superspace involve the interlayer cations (*i.e.* Ca and Ba in åkermanite and fresnoite, respectively). Bond-valence sums indicate that O atoms further apart than 3.5 Å need not be considered as bonded. This assumption implies that in the fresnoite structure, where the Ba—O bond distances do not exceed 3.4 Å, Ba is described as tenfold coordinated (Moore & Louisnathan, 1969). Looking at the modulation amplitude of the interatomic distances between Ba and the surrounding O atoms (Table 3), it is evident that the positional modulation influences especially the longest bond distances (Ba—$O3^{iv,vi}$ and Ba—$O4^{v,ix}$; symmetry codes are given in Table 3), which locally reach values higher than 3.5 Å. Thus, atoms $O3^{iv,vi}$ and $O4^{v,ix}$ locally are no longer coordinated by Ba. In particular, the maximum values observed for Ba—$O3^{iv}$ and Ba—$O4^{v}$ are 3.503 Å at $u$ = 0.34, $t$ = 0.34, and 3.553 Å at $u$ = 0.00, $t$ = 0.66, respectively (Fig. 3). Owing to this feature, eight-, nine- and tenfold coordinations of the Ba cation occur in different parts of the structure (Fig. 4). The change of coordination around the Ba atom is clearly represented by the deformation of the pentagonal rings, as seen from a projection along [001]. As observed in melilites (Kusaka *et al.*, 1998), there are deformed pentagonal rings corresponding to the cavities where the Ba atom is eight- or ninefold coordinated, and regular pentagonal rings resembling those observed in the average structure,

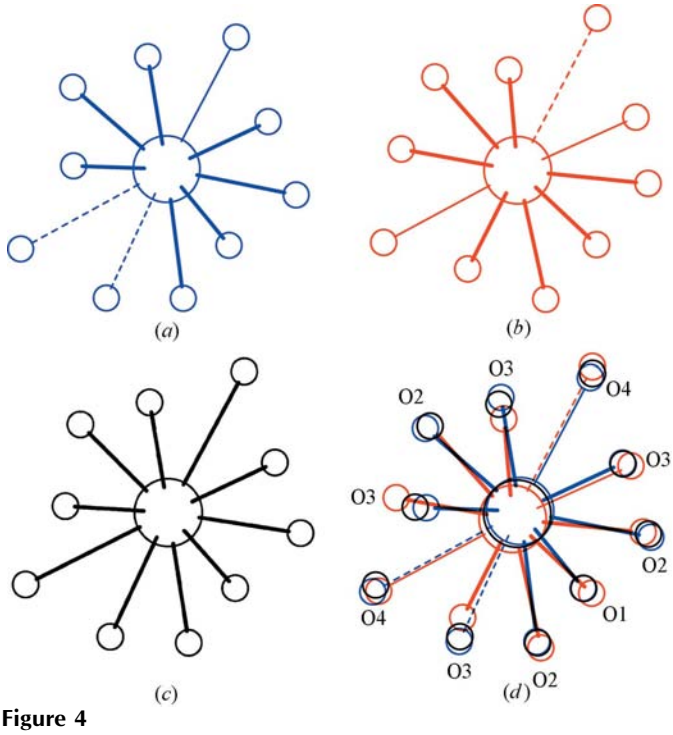


**Figure 4**
The eight- (*a*), nine- (*b*) and tenfold (*c*) coordination of barium in a view along *c*. The atomic coordinates were calculated, respectively, for $t$ = 0.266, $u$ = 0.34; $t$ = 0.671, $u$ = 0; $t$ = 0.529, $u$ = 0.34. Bonds shorter than 3 Å are denoted by a thick line; bonds above 3.4 Å are dashed. (*d*) A superposition of (*a*), (*b*) and (*c*) with bonds of the tenfold case omitted for clarity.

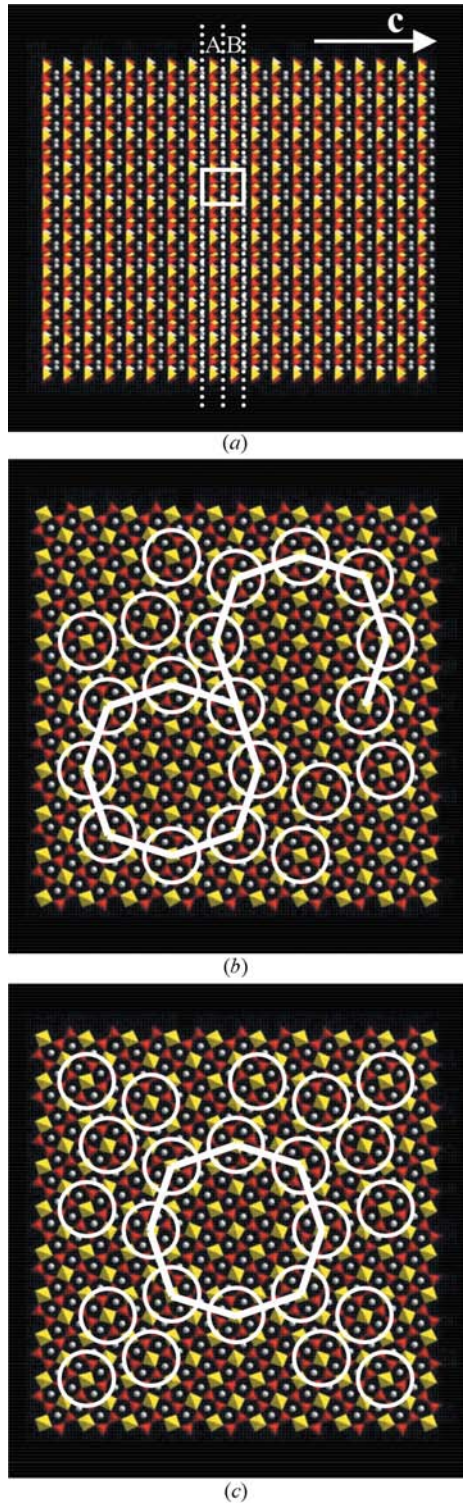


**Figure 5**
(*a*) A portion of the modulated structure of natural fresnoite projected along [100]. Triangles, squares and circles indicate Si tetrahedra, Ti pyramids and Ba cations, respectively. (*b*) Layer *A* and (*c*) layer *B* in a portion of the modulated structure of natural fresnoite projected along the *c* axis (see text). The deformed pentagonal rings hosting the Ba atoms having eight- and nine-coordinations are highlighted with a white circle. The octagonal arrangements of the deformed pentagons are indicated.

**Table 3**
The interatomic distances (Å) and angles (°) in the modulated structure of natural fresnoite.

| | Average | Minimal | Maximal |
|---|---|---|---|
| Ba—O polyhedra | | | |
| Ba—O1$^{iv}$ | 2.850 (3) | 2.733 (3) | 2.961 (3) |
| Ba—O2$^{i}$ | 2.655 (3) | 2.642 (3) | 2.672 (3) |
| Ba—O2$^{iii,v}$ | 2.797 (3) | 2.756 (3) | 2.843 (3) |
| Ba—O3$^{ii,viii}$ | 2.846 (4) | 2.729 (4) | 3.017 (4) |
| Ba—O3$^{iv,vi}$ | 3.011 (4) | 2.747 (4) | 3.503 (4) |
| Ba—O4$^{v,ix}$ | 3.344 (3) | 3.100 (3) | 3.553 (3) |
| Bond-valence sum | 1.98 (7) | 1.94 (7) | 2.03 (7) |
| Ti—$O_5$ pyramids | | | |
| Ti—O3$^{x,xi,xii,xiii}$ | 1.979 (4) | 1.962 (4) | 1.995 (4) |
| Ti—O4$^{i}$ | 1.696 (4) | 1.688 (6) | 1.703 (6) |
| O3$^{x,xii(xi,xiii)}$—Ti—O3$^{xi,xiii(x,xii)}$ | 85.4 (2) | 83.8 (2) | 86.5 (2) |
| O3$^{x(xi)}$—Ti—O3$^{xii(xiii)}$ | 147.2 (2) | 146.2 (2) | 149.4 (2) |
| O3$^{x,xi,xii,xiii}$—Ti—O4$^{i}$ | 106.4 (2) | 104.9 (2) | 107.5 (2) |
| Bond-valence sum | 3.96 (2) | 3.98 (3) | 4.00 (2) |
| Si—$O_4$ tetrahedra | | | |
| Si—O1$^{i}$ | 1.669 (3) | 1.655 (2) | 1.685 (4) |
| Si—O2$^{i}$ | 1.598 (4) | 1.597 (3) | 1.601 (3) |
| Si—O3$^{i,vii}$ | 1.623 (4) | 1.611 (4) | 1.638 (4) |
| O1$^{i}$—Si—O2$^{i}$ | 110.6 (2) | 109.9 (2) | 111.3 (2) |
| O1$^{i}$—Si—O3$^{i,vii}$ | 104.2 (2) | 102.2 (2) | 107.0 (2) |
| O2$^{i}$—Si—O3$^{i,vii}$ | 115.1 (2) | 114.1 (2) | 115.8 (2) |
| O3$^{i}$—Si—O3$^{vii}$ | 106.6 (2) | 105.5 (2) | 107.5 (2) |
| Bond-valence sum | 4.16 (2) | 4.09 (2) | 4.24 (2) |

Symmetry codes: (i) $x, y, z$; (ii) $x, y, -\frac{1}{2}+z$; (iii) $-y, -1+x, z$; (iv) $-y, -1+x, -\frac{1}{2}+z$; (v) $\frac{1}{2}-x, -\frac{1}{2}+y, z$; (vi) $\frac{1}{2}-x, -\frac{1}{2}+y, -\frac{1}{2}+z$; (vii) $-\frac{1}{2}-y, -\frac{1}{2}-x, z$; (viii) $-\frac{1}{2}-y, -\frac{1}{2}-x, -\frac{1}{2}+z$; (ix) $x, -1+y, z$; (x) $\frac{1}{2}-x, \frac{1}{2}+y, z$; (xi) $-\frac{1}{2}-y, \frac{1}{2}-x, z$; (xii) $-\frac{1}{2}+x, -\frac{1}{2}-y, z$; (xiii) $\frac{1}{2}+y, -\frac{1}{2}+x, z$. The bond-valence sums were calculated according to Brown & Altermatt (1985).

which correspond to tenfold Ba coordinations. To investigate the distribution of the deformed pentagonal rings, a portion of the modulated structure of natural fresnoite was built as a function of the fourth and the fifth coordinate of the superspace (Fig. 5). It should be stressed that the incommensurate satellites possess a $c^*/2$ commensurate component. This feature implies that in the incommensurate structure two different layers (labelled *A* and *B* in Fig. 5*a*) are stacked along the *c* axis. A careful analysis of both the *A* and the *B* single layers projected along the *c* axis (Figs. 5*b* and 5*c*) shows two types of distribution of deformed pentagonal rings (highlighted with a circle in Figs. 5*b* and 5*c*). Most of them form octagonal clusters closely resembling those observed in the IC structures of both natural (Bindi *et al.*, 2001) and synthetic melilite-type compounds (Kusaka *et al.*, 1998, 2001). Nonetheless, in the melilite-type compounds the octagonal clusters of deformed pentagons surround flattened *T*1 tetrahedra, whereas in fresnoite the $TiO_5$ pyramids are always quite regular. The Ti—O bond lengths and O—Ti—O angles (Table 3), indeed, are virtually unaffected by the modulation, their variations being within or close to the experimental uncertainties, respectively. The $TiO_5$ pyramids essentially rotate around their *c* axes and it is found that the pyramids belonging to subsequent layers move slightly off phase. A similar behaviour was observed for the modulated structure of the BTG compound (Höche *et al.*, 2003). In addition, the modulation of the Si tetrahedron has an essentially rotational

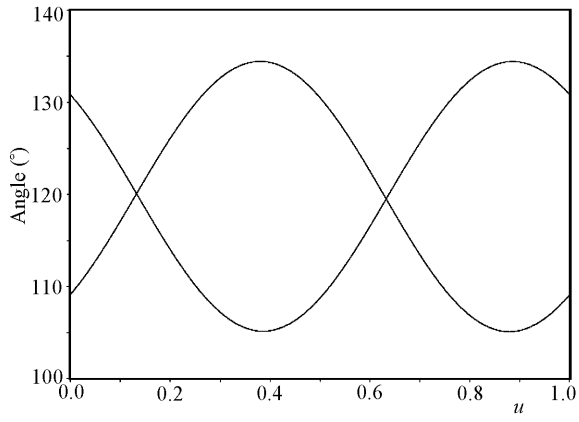


**Figure 6**
Variation of the O3$^{i}$—O1$^{i}$—O3$^{i,vii}$ angles as functions of $u$ at $t$ = 0.0. (Symmetry codes as in Table 3.)

character. The tetrahedral external shape does not change significantly as a function of $t$ and $u$ coordinates. More pronounced variations, however, affect the O—Si—O angles (Table 3). The change of the geometry of the pyrosilicate group is made evident by the strong variation of the O3$^{i}$—O1$^{i}$—O3$^{i,vii}$ angles (Fig. 6) ranging from 134.5° at $u$ = 0.38 to 105.0° at $u$ = 0.88.

Finally, the role of the chemical composition in the stabilization of the incommensurate phase deserves to be discussed. As far the synthetic melilite-type compounds are concerned, geometrical restrictions exist in terms of the size of the tetrahedral cations with respect to the size of the interlayer *X* cations (Seifert *et al.*, 1987; Röthlisberger *et al.*, 1990). The greater the size of the tetrahedra with respect to the *X* polyhedra, the greater the structural misfit leading to the incommensurate structure. Therefore, a modulation occurs when divalent cations such as Mg, $Fe^{2+}$, Co and Zn fill the *T*1 site with Ca occupying the *X* site. Conversely, IC satellites are not observed when larger numbers of smaller cations enter the tetrahedral sites. A comparison between what is observed in the present crystal and in the synthetic $Ba_2TiGe_2O_8$ structure (Höche *et al.*, 2003), which exhibits a closely related but orthorhombic structure, suggests that the stabilization of the incommensurate structure in fresnoite-type compounds is ruled by an analogous mechanism. Where the tetrahedral site is occupied by a larger cation (*i.e.* Ge), the modulation amplitude of the Ba—O distances increases. The longest Ba—O distances, in fact, locally reach values even higher than 4 Å. In other words, this corresponds to a higher percentage of eight- and ninefold coordination polyhedra around Ba and, therefore, of deformed pentagonal rings. A comparative description in terms of large-scale regularity in fresnoites, however, would require that the incommensurately modulated structures of compounds exhibiting a wide range of chemical composition be fully described in terms of superspace representation.

The authors are grateful to Filippo Olmi (CNR Istituto di Geoscienze e Georisorse, Sezione di Firenze, Italy) for his

help in electron microprobe analyses and to Ray Withers (Australian National University, Canberra, Australia) for the reading of the final version of the manuscript. LB and PB acknowledge CNR (Istituto di Geoscienze e Georisorse, Sezione di Firenze) and MIUR, PRIN 2005 project 'Complexity in minerals: modulation, modularity, structural disorder', issued to Silvio Menchetti. MD and VP gratefully acknowledge the support of the Grant Agency of the Czech Republic, projects 202/05/0421 (measurement) and 202/06/0757 (calculation).

## References

Bindi, L., Bonazzi, P., Dusek, M., Petricek, V. & Chapuis, G. (2001). *Acta Cryst.* B**57**, 739–746.
Brown, I. D. & Altermatt, D. (1985). *Acta Cryst.* B**41**, 244–247.
Burla, M. C., Camalli, M., Carrozzini, B., Cascarano, G. L., Giacovazzo, C., Polidori, G. & Spagna, R. (2003). *J. Appl. Cryst.* **36**, 1103.
Choi, J., Zhu, Z. T., Musfeldt, J. L., Ragghianti, G., Mandrus, D., Sales, B. C. & Thompson, J. R. (2002). *Phys. Rev. B*, **65**, 054101.
Flack, H. D. (1983). *Acta Cryst.* A**39**, 876–881.
Halliyal, A., Bhalla, A. S., Markgraf, S. A., Cross, L. E. & Newnham, R. E. (1985). *Ferroelectrics*, **62**, 27–38.
Höche, T., Esmaeilzadeh, S., Uecker, R., Lidin, S. & Neumann, W. (2003). *Acta Cryst.* B**59**, 209–216.
Höche, T., Neumann, W., Esmaeilzadeh, S., Uecker, R., Lentzen, M. & Rüssel, C. (2002). *J. Solid State Chem.* **166**, 15–23.
Höche, T., Rüssel, C. & Neumann, W. (1999). *Solid State Commun.* **110**, 651–656.
Iijima, K., Marumo, F., Kimura, M. & Kawamura, T. (1981). *J. Chem. Soc. Jpn*, **10**, 1557–1563.
Kimura, M., Doi, S., Nanamatsu, S. & Kawamura, T. (1973). *Appl. Phys. Lett.* **10**, 531–532.
Kusaka, K., Hagiya, K., Ohmasa, M., Okano, Y., Mukai, M., Iishi, K. & Haga, N. (2001). *Phys. Chem. Miner.* **28**, 150–166.
Kusaka, K., Ohmasa, M., Hagiya, K., Iishi, K. & Haga, N. (1998). *Mineral. J.* **20**, 47–58.
Liu, G. & Greedan, J. E. (1995). *J. Solid State Chem.* **114**, 499–505.
Markgraf, S. A. & Bhalla, A. S. (1989). *Phase Transit.* **18**, 55–76.
Markgraf, S. A., Halliyal, A., Bhalla, A. S. & Newnham, R. E. (1985). *Ferroelectrics*, **62**, 17–26.
Markgraf, S. A., Randall, C. A., Bhalla, A. S. & Reeder, R. J. (1990). *Solid State Commun.* **75**, 821–824.
Masse, R., Grenier, J. C. & Durif, A. (1967). *Bull. Mineral.* **90**, 20–23.
Moore, P. B. & Louisnathan, J. (1969). *Z. Kristallogr.* **130**, 438–448.
Oxford Diffraction (2004). *CrysAlisPro CCD* and *CrysAlisPro RED*. Oxford Diffraction Ltd, Abingdon, Oxford, England.
Petricek, V., Dusek, M. & Palatinus, L. (2000). *JANA2000.* Institute of Physics, Academy of Sciences of the Czech Republic, Prague, Czech Republic.
Röthlisberger, F., Seifert, F. & Czank, M. (1990). *Eur. J. Mineral.* **2**, 585–594.
Schmid, H., Genequand, P., Tippmann, H., Pouilly, G. & Guedu, H. (1978). *J. Mater. Sci.* **13**, 2257–2265.
Seifert, F., Czank, M., Simons, B. & Schmahl, W. (1987). *Phys. Chem. Miner.* **14**, 26–35.
Withers, R. L., Höche, T., Liu, Y., Esmaeilzadeh, S., Keding, R. & Sales, B. (2004). *J. Solid State Chem.* **177**, 3316–3323.
Withers, R. L., Tabira, Y., Liu, Y. & Höche, T. (2002). *Phys. Chem. Miner.* **29**, 624–632.
Wolff, P. M. de (1974). *Acta Cryst.* A**30**, 777–785.
Ye, N., Chen, Q., Wu, B. & Chen, C. (1998). *J. Appl. Phys.* **84**, 555–558.